Gap structure of the local field in symmetric Q Ising neural networks

D. Bollé[1,*] and G. M. Shim[2,†]
[1]*Instituut voor Theoretische Fysica, Katholieke Universiteit Leuven, B-3001 Leuven, Belgium*
[2]*Department of Physics, Chungnam National University, Yuseong, Taejon 305-764, Republic of Korea*
(Received 13 February 2002; published 7 June 2002)

The time evolution of the local field in *symmetric* Q-Ising neural networks is studied for arbitrary Q. In particular, the structure of the noise and the appearance of gaps in the probability distribution are discussed. Results are presented for several values of Q and compared with numerical simulations.

DOI: 10.1103/PhysRevE.65.067101 PACS number(s): 64.60.Cn, 02.50.−r, 87.10.+e

In a number of papers in the 1990s (cf. [1–10] and references therein) the parallel dynamics of Q-Ising type neural networks has been discussed for several architectures using a probabilistic approach. For the asymmetric extremely diluted and layered architectures this dynamics can be solved exactly and it is known that the local field only contains Gaussian noise. For networks with symmetric connections, however, things are quite different. Even for extremely diluted versions of these systems feedback correlations become essential, complicating the dynamics in a nontrivial way.

Only recently, a complete solution has been obtained for the dynamics of symmetric Q-Ising networks at zero temperature, taking into account all feedback correlations [9,10]. Thereby, it is seen that both for the fully connected (FC) and the symmetric extremely diluted (SED) architectures, the local field contains a discrete and a Gaussian noise part. This discrete part prevents a closed-form solution of the dynamics but a recursive scheme can be developed in order to calculate the complete time evolution of the order parameters.

Since the local field is a basic ingredient of the recursive scheme, it is interesting by itself to study its probability distribution. Moreover, once this distribution is known, many properties of the network, in particular the order parameters themselves, can be calculated. The stability of the retrieval phase is also reflected in a gap structure of the distribution. A better check of the theory can be provided by comparing directly the local field instead of the macroscopic order parameters, with simulations.

In more detail, we want to see how the initial Gaussian behavior at time zero evolves, especially under the presence of discrete noise. Next, we also want to find out whether the specific structure of the architecture (FC or SED), the value of Q, and the fact whether we are in a retrieval region or not, changes the behavior of the distribution. Finally, numerical simulations are performed confirming the analytic study and giving additional insight into the behavior of the local field.

Consider a neural network of N neurons, which can take values σ_i from a discrete set $\{-1=s_1<\cdots<s_Q=+1\}$. The p patterns to be stored in this network are supposed to be a collection of independent and identically distributed random variables (IIDRV), ξ_i^μ, $\mu=1,\ldots,p$, with zero mean and variance A. The latter is a measure for the activity of the patterns. Given the configuration $\boldsymbol{\sigma}(t)\equiv\{\sigma_i(t)\}$, the local field in neuron i equals

$$h_i(\boldsymbol{\sigma}(t))\equiv h_i(t)=\sum_j J_{ij}(t)\sigma_j(t), \tag{1}$$

with J_{ij} the synaptic coupling. For the SED and the FC architectures the couplings are given by the Hebb rule

$$J_{ij}^{SED}=\frac{c_{ij}}{CA}\sum_\mu \xi_i^\mu\xi_j^\mu \quad \text{for} \quad i\neq j, \quad J_{ii}^{SED}=0, \tag{2}$$

$$J_{ij}^{FC}=\frac{1}{NA}\sum_\mu \xi_i^\mu\xi_j^\mu \quad \text{for} \quad i\neq j, \quad J_{ii}^{FC}=0, \tag{3}$$

with the $c_{ij}=c_{ji}=0,1$ chosen to be IIDRV with distribution $\Pr\{c_{ij}=x\}=(1-C/N)\delta_{x,0}+(C/N)\delta_{x,1}$. Thereby, it is assumed that $C\ll\ln N$. For the SED model the architecture is a local Cayley tree but, in contrast with the diluted asymmetric model, it is no longer directed such that it causes a feedback from $t\geqslant 2$ onwards.

At zero temperature all neurons are updated in parallel according to the rule

$$\sigma_i(t+1)=g_b(h_i(t)),$$

$$g_b(x)\equiv\sum_{k=1}^{Q} s_k\{\theta[b(s_{k+1}+s_k)-x]-\theta[b(s_k+s_{k-1})-x]\}, \tag{4}$$

with $s_0\equiv-\infty$ and $s_{Q+1}\equiv+\infty$. Here $g_b(\cdot)$ is the gain function and $b>0$ is the gain parameter of the system.

In order to measure the retrieval quality one can use the Hamming distance between a stored pattern and the microscopic state of the network. This introduces the main overlap and the arithmetic mean of the neuron activities

$$m_N^\mu(t)=\frac{1}{NA}\sum_i \xi_i^\mu\sigma_i(t), \quad a_N(t)=\frac{1}{N}\sum_i [\sigma_i(t)]^2. \tag{5}$$

The key question is then how these quantities evolve in time. One finds from Eq. (4) using the law of large numbers that in the thermodynamic limit

*Email address: desire.bolle@fys.kuleuven.ac.be
†Email address: gmshim@cnu.ac.kr

$$m^1(t+1)=\frac{1}{A}\langle\langle \xi_i^1 g_b(h_i(t))\rangle\rangle, \quad a(t+1)=\langle\langle g_b^2(h_i(t))\rangle\rangle. \tag{6}$$

In the above $\langle\langle\cdot\rangle\rangle$ denotes the average both over the distribution of the embedded patterns ξ_i^μ and the initial configurations $\sigma_i(0)$. The average over the latter is hidden in an average over $h_i(t)$ through Eq. (4). We remark that for the SED model the thermodynamic limit contains both $C\to\infty$ and $N\to\infty$. Furthermore, all averages have to be taken over the treelike structure, and the capacity $\alpha=p/N$ has to be replaced by $\alpha=p/C$.

In Eq. (6), $h_i(t)$ is the main ingredient. Employing a probabilistic signal-to-noise ratio analysis it has been shown that, for a general time step t, $h_i(t)$ is given by [9,10]

$$h_i(t)=\xi_i^1 m^1(t)+\mathcal{N}(0,\alpha a(t))+\chi(t-1)\{F[h_i(t-1)-\xi_i^1 m^1(t-1)]+\alpha\sigma_i(t-1)\}, \tag{7}$$

where $F=1$ for the FC architecture and $F=0$ for the SED one. So, the local field at time t consists out of a discrete part and a Gaussian distributed part

$$h_i(t)=M_i(t)+\mathcal{N}(0,V(t)), \tag{8}$$

where $M_i(t)$ consists out of a signal term and a discrete noise term

$$M_i(t)=\xi_i^1 m^1(t)+\alpha\chi(t-1)\sigma_i(t-1)+F\sum_{t'=0}^{t-2}\alpha\left[\prod_{s=t'}^{t-1}\chi(s)\right]\sigma_i(t') \tag{9}$$

and a recursion relation for $V(t)$ can be obtained from Eq. (7). Since we do not need it explicitly in the sequel we do not write it down. The quantity $\chi(t)$ reads

$$\chi(t)=\sum_{k=1}^{Q-1} f_{h_i^\mu(t)}[b(s_{k+1}+s_k)](s_{k+1}-s_k), \tag{10}$$

with $f_{h_i^\mu(t)}$ the probability density of $h_i^\mu(t)$ in the thermodynamic limit. Since different architectures contain different correlations not all terms in these final equations are present, as is apparent through F. We remark that for the asymmetric diluted and the layered feedforward architecture $M_i(t)=\xi_i^1 m^1(t)$ so that in these cases the local field consists out of a signal term plus Gaussian noise for *all* time steps [6,7].

For the architectures treated here we still have to determine the probability density $f_{h_i(t)}$ in Eq. (10). This can be done by looking at the form of $M_i(t)$ given by Eq. (9). The evolution equation tells us that $\sigma_i(t')$ can be replaced by $g_b(h_i(t'-1))$ such that the second and third terms of $M_i(t)$ are the sums of step functions of correlated variables. These are also correlated through the dynamics with the Gaussian distributed part of $h_i(t)$. Therefore, the local field can be considered as a transformation of a set of correlated Gaussian variables x_s, which we choose to normalize. Defining the correlation matrix $W=(E[x_s x_{s'}])$ we arrive at the following expression for $f_{h_i(t)}$ for the FC model:

$$f_{h_i(t)}(y)=\int dx_t\prod_{s=0}^{t-2} dx_s\,\delta(y-M_i(t)-\sqrt{V(t)}x_t)\times\frac{1}{\sqrt{\det(2\pi W)}}\exp\left(-\frac{\mathbf{x}W^{-1}\mathbf{x}^T}{2}\right), \tag{11}$$

with $\mathbf{x}=\{x_s\}=(x_0,\ldots,x_{t-2},x_t)$. For the symmetric diluted case this expression simplifies to

$$f_{h_i(t)}(y)=\int\prod_{s=0}^{[t/2]} dx_{t-2s}\frac{1}{\sqrt{\det(2\pi W)}}\exp\left(-\frac{\mathbf{x}W^{-1}\mathbf{x}^T}{2}\right)\delta\times(y-\xi_i^1 m^1(t)-\alpha\chi(t-1)\sigma_i(t-1)-\sqrt{\alpha a(t)}x_t), \tag{12}$$

with $\mathbf{x}=(\{x_s\})=(x_{t-2[t/2]},\ldots,x_{t-2},x_t)$. The brackets $[t/2]$ denote the integer part of $t/2$.

The equilibrium distribution of $h_i(t)$ can be obtained by eliminating the time dependence in (7)

$$h_i=\xi_i^1 m^1+\eta\mathcal{N}(0,\alpha a)+\alpha\chi\eta\sigma_i, \tag{13}$$

with $\eta=1/(1-\chi)$ for the FC architecture and $\eta=1$ for the SED one. The corresponding updating rule (4)

$$\sigma_i=g_b(\tilde{h}_i+\alpha\chi\eta\sigma_i), \quad \tilde{h}_i=\xi_i^1 m_i^1+\eta\mathcal{N}(0,\alpha a) \tag{14}$$

in general admits more than one solution. A Maxwell construction (see, e.g., Refs. [9–11]) can be made leading to a unique solution

$$\sigma_i=g_{\tilde{b}}(\widetilde{h_i}), \quad \tilde{b}=\left(b-\frac{\alpha\eta\chi}{2}\right) \tag{15}$$

such that we have $\sigma_i=s_k$ if $\tilde{b}(s_k+s_{k-1})+\alpha\chi\eta s_k<h_i<\tilde{b}(s_k+s_{k+1})+\alpha\chi\eta s_k$ for $\tilde{b}>0$ and $\sigma_i=\pm 1$ if $\pm h_i>\alpha\eta\chi$ for $\tilde{b}<0$. This unique solution can be used to obtain fixed-point equations for the main overlap and activity (6). Those equations are equal to those derived from a thermodynamic replica-symmetric mean-field theory approach [12,13]. For analog networks ($Q\to\infty$) such a Maxwell construction is not necessary because Eq. (14) has only one solution.

Next, we calculate the probability density of the local field by plugging these results into Eq. (13) to obtain, forgetting about the site index i and the pattern index 1,

$$f(h)=\sum_{k=1}^{Q}\frac{1}{\eta\sqrt{2\pi\alpha a}}\exp\left(-\frac{(h-\xi m-\alpha\chi\eta s_k)^2}{2\alpha a\eta^2}\right)\times\{\theta[\tilde{b}(s_k+s_{k+1})+\alpha\chi\eta s_k-h]-\theta[\tilde{b}(s_k+s_{k-1})+\alpha\chi\eta s_k-h]\}, \tag{16}$$

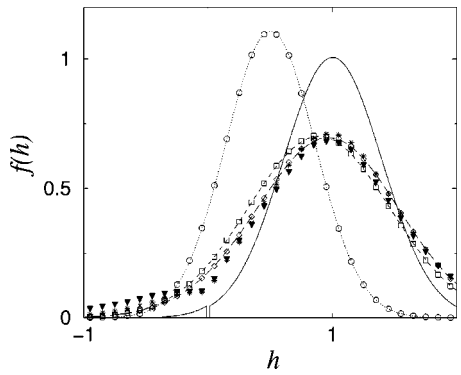

FIG. 1. A comparison of theoretical results and numerical simulations with $N=6000$ for $f(h)$ of a retrieval state in the $Q=2$ system with $\alpha=0.13$, $m_0=0.5$. Theoretical (simulation) results for $t=0,1,2$ are indicated by a dotted curve (circles), a short-dashed curve (squares), and a long-dashed curve (diamonds). Simulations for $t=10,20$ (stars, triangles) are shown and the solid curve presents the equilibrium distribution.

meaning that $(Q-1)$ gaps occur, respectively, at $\tilde{b}(s_k+s_{k-1})+\alpha\chi\eta s_{k-1}<h<\tilde{b}(s_k+s_{k+1})+\alpha\chi\eta s_k$ with width $\Delta h=2\alpha\chi\eta/(Q-1)$. For analog networks no gaps occur. When $\tilde{b}\leqslant 0$ the effective gain function (15) becomes two-state Ising-like such that in that case only one gap occurs.

For $Q=2$ this expression (16) simplifies to

$$f(h)=\frac{\theta(h-\alpha\chi\eta)}{\eta\sqrt{2\pi\alpha a}}\exp\left(-\frac{(h-\xi m-\alpha\chi\eta)^2}{2\alpha a\eta^2}\right)+\frac{\theta(-h-\alpha\chi\eta)}{\eta\sqrt{2\pi\alpha a}}\exp\left(-\frac{(h-\xi m+\alpha\chi\eta)^2}{2\alpha a\eta^2}\right). \tag{17}$$

This result is consistent with the gap in the internal-field distribution for an infinite range spin glass found by a Bethe-Peierls-Weiss approach [14] (see also Refs. [15,16]). It is straightforward to work out a similar formula for bigger values of Q.

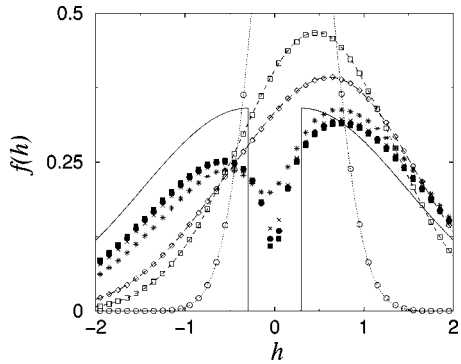

FIG. 2. As in Fig. 1, for a $Q=2$ nonretrieval spin-glass state with $\alpha=0.14$, $m_0=0.2$. Further simulations for $t=10$ (stars), $t=30$ (crosses), $t=50$ (filled circles), and $t=100$ (filled squares) are shown.

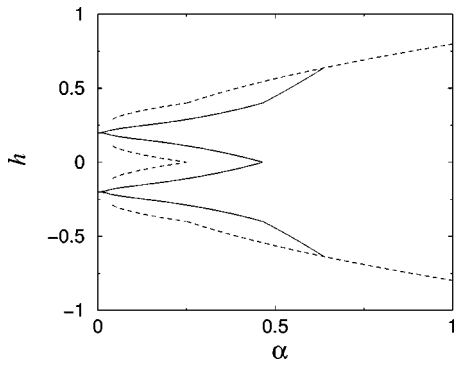

FIG. 3. The gap boundaries in h as a function of α for retrieval (solid curve) and nonretrieval (dashed curve) states for the $Q=3$ SED systems with $b=0.2$.

We have investigated these probability distributions numerically using the corresponding fixed-point equations mentioned before, for several values of Q and compared them with those obtained from numerical simulations of the dynamics for networks of $N=6000$ neurons. Some typical results are shown in Figs. 1–4.

In Figs. 1 and 2 the local field distribution for the fully connected $Q=2$ network is shown for a retrieval state ($\alpha=0.13$, $m_0=0.5$) just below the critical capacity and a nonretrieval spin-glass state ($\alpha=0.14$, $m_0=0.2$) just above it. Both the first few time steps and the equilibrium result derived above are compared with numerical simulations. They are in agreement. For the retrieval state there is, typically, a small gap in the equilibrium distribution around $h=0$. For small α the gap is very narrow. Furthermore, in the simulations one sees that this gap shows up very quickly. For the nonretrieval state the gap is typically much bigger. Again in the simulations one quickly sees the gap but it is extremely difficult numerically to find points touching the zero axis because of finite size effects.

We find that the gap width at equilibrium, Δh, for the nonretrieval state as a function of Q with $b=0.5$ scales as $\Delta h\sim 1/(Q-1)$ and, hence, decreases to zero for $Q\to\infty$. This constant behavior of $(Q-1)\Delta h$ attains already for values of

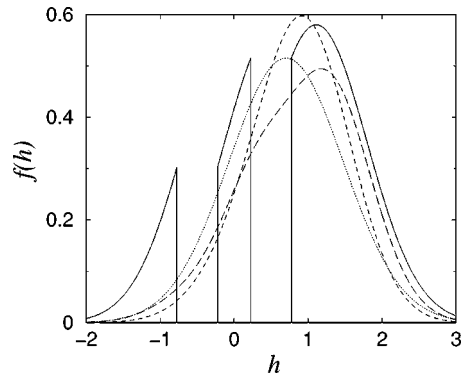

FIG. 4. The local field distribution $f(h)$ of a retrieval state for pattern values $+1$ in the SED $Q=3$ system with $\alpha=0.6$, $b=0.5$, $m_0=0.7$. Results for $t=0$, 1, 2, and ∞ are indicated by a dotted curve, a short-dashed curve, a long-dashed curve, and a solid curve, respectively.

$Q \geqslant 20$ and is also seen for the retrieval state. These results are insensitive to the structure of the symmetric architecture.

In Fig. 3 the gap boundaries in h as a function of α are compared for retrieval and non-retrieval states in the SED $Q=3$, $b=0.2$ model. We remark that in this case the spin-glass states do not exist for $\alpha \leqslant 0.04$ [13] so that there is no gap for these α values. For α large enough ($\alpha > 0.465$ for retrieval states and $\alpha > 0.252$ for spin-glass states) there exists one gap only since the effective gain function becomes Ising-like [13]. More gaps with smaller widths are formed when increasing Q for both the fully connected and diluted models. For $Q \to \infty$ the gaps disappear.

Comparing the gaps for the spin-glass states in the FC and SED $Q=3$ models with $b=0.5$ we find that for $\alpha \leqslant 0.25$ there exist no spin-glass states in the SED model [13] and for $\alpha \leqslant 0.004$ there are none in the FC model [12]. When both do exist the gap widths are almost equal. So the dilution has some influence on the existence of the gap but, again, not on its width.

Finally, Fig. 4 presents the local field distribution for the SED $Q=3$, $b=0.5$ model for a retrieval state ($\alpha=0.6$, $m_0=0.7$) just below the critical capacity. Only the distribution with pattern values $+1$ is shown. It is asymmetric and two gaps are found at equilibrium. For pattern values 0 the distribution is symmetric and the gap locations and widths are the same [see Eq. (16)] but their height is different.

In conclusion, we have studied the time evolution of the local field in symmetric Q-Ising neural networks both in the retrieval and spin-glass regime. We have found a gap structure in its probability distribution depending on the specific architecture and on the value of Q. The most important findings are that dilution changes the region of existence of the gap but not its width and that the gap becomes typically much bigger when we cross the retrieval transition line into the spin-glass region. These results agree with numerical simulations.

This work has been supported in part by the Fund for Scientific Research, Flanders-Belgium and the Korea Science and Engineering Foundation through the SRC program. The authors are indebted to A. Coolen, G. Jongen, and V. Zagrebnov for constructive discussions.

[1] A. E. Patrick and V. A. Zagrebnov, J. Phys. A **23**, L1323 (1990); **25**, 1009 (1992).
[2] A. E. Patrick and V. A. Zagrebnov, J. Stat. Phys. **63**, 59 (1991).
[3] T. L. H. Watkin and D. Sherrington, J. Phys. A **24**, 5427 (1991).
[4] A. E. Patrick and V. A. Zagrebnov, J. Phys. A **24**, 3413 (1991).
[5] D. Bollé, B. Vinck, and V. A. Zagrebnov, J. Stat. Phys. **70**, 1099 (1993).
[6] D. Bollé, G. M. Shim, B. Vinck, and V. A. Zagrebnov, J. Stat. Phys. **74**, 565 (1994).
[7] D. Bollé, G. M. Shim, and B. Vinck, J. Stat. Phys. **74**, 583 (1994).
[8] D. Gandolfo, M. Sirugue-Collin, and V. A. Zagrebnov, Network Comput. Neural Syst. **9**, 563 (1998).
[9] D. Bollé, G. Jongen, and G. M. Shim, J. Stat. Phys. **91**, 125 (1998).
[10] D. Bollé, G. Jongen, and G. M. Shim, J. Stat. Phys. **96**, 861 (1999).
[11] M. Shiino and T. Fukai, Phys. Rev. E **48**, 867 (1993).
[12] D. Bollé, H. Rieger, and G. M. Shim, J. Phys. A **27**, 3411 (1994).
[13] D. Bollé, D. Carlucci, and G. M. Shim, J. Phys. A **33**, 6481 (2000).
[14] L. J. Schowalter and M. W. Klein, J. Phys. C **12**, L935 (1979).
[15] V. A. Zagrebnov and A. S. Chvyrov, Sov. Phys. JETP **68**, 153 (1989).
[16] A. C. C. Coolen and D. Sherrington, Phys. Rev. E **49**, 1921 (1994).